Cell Proliferation

Cell Prolif., 2016, **49**, 36–47 doi: 10.1111/cpr.12236

Overexpression of CD61 promotes hUC-MSC differentiation into male germ-like cells

Bo Li*,[a], Weishuai Liu†,[a], Mengru Zhuang*, Na Li*, Siyu Wu*, Shaohui Pan* and Jinlian Hua*

**College of Veterinary Medicine, Shaanxi Centre of Stem Cells Engineering & Technology, Northwest A&F University, Yangling, Shaanxi 712100, China and †Department of Pathology, Yangling Demonstration Zone Hospital, Yangling, Shaanxi 712100, China*

Received 24 August 2015; revision accepted 6 October 2015

Abstract

Objectives: Previous studies have shown that germ-like cells can be induced from human umbilical cord mesenchymal stem cell (hUC-MSCs) *in vitro*. However, induction efficiency was low and a stable system had not been built. CD61, also called integrin-β3, plays a significant role in cell differentiation, in that CD61-positive-cell-derived pluripotent stem cells easily differentiate into primordial germ-like cells (PGC). Here, we have explored whether overexpression of CD61 would promote hUC-MSC differentiation into PGC and male germ-like cells.

Materials and methods: hUC-MSCs were cultured and transduced using pCD61-CAGG-TRIP-pur (oCD61) and pTRIP-CAGG plasmid (Control), and hUC-MSCs overexpressed CD61 were induced by bone morphogenetic protein 4 (BMP4, 12.5 ng/ml), to differentiate into PGC and male germ cells. Quantitative real-time PCR (RT-qPCR), western blotting and immunofluorescence staining were used to examine PGC- and germ cell-specific markers.

Results: High expression levels of PGC-specific markers were detected in oCD61 hUC-MSCs compared to controls. After BMP4 induction, expression levels of male germ cell markers such as Acrosin (ACR), Prm1 and meiotic markers including Stra8, Scp3 in oCD61 were significantly higher than those of the Control group.

Conclusions: Under induction of BMP4, CD61-overexpressing hUC-MSCs, which had turned into PGC-like cells, could be further differentiated into male germ-like cells. Thus, a simple and efficient approach to study male germ cell development by using hUC-MSCs has been established.

Correspondence: J. Hua, College of Veterinary Medicine, Shaanxi Centre of Stem Cells Engineering & Technology, Northwest A&F University, Yangling, Shaanxi 712100, China. Tel.: 86-29-87080068; Fax: 86-29-87080068; E-mail: jinlianhua@nwsuaf.edu.cn

[a]These authors contributed equally to this work.

Introduction

Reproductive health recieves more and more attention in today's society. Incidence of infertility is in the order of 8–12% of couples of childbearing age, in whom occurrence of problems caused by the male account for 40% to 50% (1). It is difficult to cure male infertility as its factors are very complex, and deficiencies in semen are a common symptom. Human spermatogenesis is a long and precise process including spermatogonial stem cell (SSC) self-renewal, meiosis of spermatocytes and sperm maturation. Recent studies have suggested that the transplantation of stem cells – SSCs, embryonic stem cells (ESCs), induced pluripotent stem cells (iPSCs) or mesenchymal stem cell (MSCs) could be viewed as promising methods for thoroughly curing male infertility (2–7).

Mesenchymal stem cells can be found in a variety of tissues, and are equipped with high capacities for self-renewal and potency of differentiation. They have the potential to differentiate into varieties of cells, including adipose, nervous and myocardial ones (8–10). Recent studies have shown that mouse and human bone marrow-derived MSCs can differentiate into artificial "gametes (sperm or oocyte)" both *in vivo* and *in vitro* (11,12). However, differentiation potential and number of bone marrow-derived MSCs tend to reduce gradually with aging of the donor. Thus, many scientists are enthusiastic to find alternative sources of MSCs. Recent evidence has shown that human umbilical cord mesenchymal stem cells (hUC-MSCs) are positive for MSC surface markers CD29, CD44, CD59, CD105, negative or weak for CD14, CD28, CD33, CD34, CD45, CD117, and markers associated with cell transplantation rejection

such as CD40, CD80 and CD86 also are weakly expressed (8). The cells have the capability to differentiate into cells of bone, cartilage and adipose tissues (13–15).

CD61, also known as integrin-β3, is a variety of adhesion receptor, widely distributed on surfaces of cells, participating in cell signalling pathways of molecular and protein information transmission, across cell membranes, to regulate bodily physiology. Some scientists have found that it plays a key role in embryonic development, immunological responses (16) and sperm maturation (17). Integrin-β3- and SSEA-1-positive cells are very similar with BV (Blimp and Stella) positive (15). Integrin-β3 and SSEA-1 have been identified as markers for isolation of PGCLCs (PGC-like cells) with spermatogenic capacity, from differentiated pluripotent stem cells (3,4). BMP4 plays a regulatory role in PGC migration and specification processes (19). Mouse and human embryonic stem cells can successfully differentiate into PGCs by induction of BMP4 (4), however, the mechanism is not clear and in experiments efficiency was low. As previous studies have demonstrated, both BMP4 and retinoic acid (RA) can induce PGCs to express some early male germ cell-specific markers (13,20).

CD61 is vital for PGCs with spermatogenic capacity in mouse (4). However, there is little information on the mechanisms of its effects on germ cell development. In the study described here, human CD61 was cloned and its characteristics were analysed using bioinformatics software and websites. Then we investigated effects of overexpression of CD61 in combination with BMP4, on hUC-MSCs.

Materials and methods

Isolation and culture of hUC-MSCs

hUC-MSCs were obtained from our laboratory (13), and cells were cultured in DMEM/F12 (Invitrogen, Carlsbad, CA, USA) supplemented with 15% foetal bovine serum (FBS, Hyclone, Logan, UT, USA), 0.1 mM 2-mercaptoethanol (Invitrogen), 2 mM Glutamine (Invitrogen), 1% non-essential amino acids (Invitrogen), under humidified conditions at 37 °C with 5% CO_2. Culture plates were pre-treated with 0.1% gelatin overnight, and cells were passaged every 2–3 days.

Construction of recombination plasmid

The *CD61* gene was amplified from umbilical cords by PCR with Phanta Super-Fidelity DNA Polymerase (Vazyme Biotech, Beijing, China). Primers were synthesized by Sangon Biotech (Shanghai, China), and forward: 5′-AAGCTAGCATGCGAGCGCGGCCG-3′; reverse: 5′-CGCTCGAGCGTGGCACAGGCTGATAAT-3’. The product is 2409 bp. PCR products were analysed by 1.5% agarose (Invitrogen) gel electrophoresis, stained with ethidium bromide (Invitrogen), and visualized under UV illumination (15,21). Amplification was cloned into pMD18-T prokaryotic expression vector (TaKaRa, Shanghai, China). After white-blue screening, positive clones were confirmed by PCR, dual restriction enzyme digestion and sequencing. Then, specific amplified fragments were cloned into pTRIP-CAGG-pur Lentiviral expression vector to obtain pCD61-CAGG-TRIP-pur recombination plasmid. The plasmid was validated by PCR and restriction enzyme digestion.

Alignment and evolutionary relationship of CD61 CDS

The fragment of human CD61 was cloned by RT-PCR and sequenced by Sangon Biotech (Shanghai, China). Sequences in this study were all from NCBI (websites in this study are all listed in Table 1). Sequences were aligned and the phylogenetic tree was depicted using DNAMAN software. Location of human *CD61* gene was identified by blasting on NCBI.

Nc values, CBI and CAI, and Ka/Ks calculation

Nc values were obtained from Emboss Nc value by typing the sequence. CAI was obtained from Emboss CAI by the same method. Calculation of CBI needs the cusp of 12 species, the cusp of each being obtained from Emboss cusp. Then we calculated CBI by Matlab soft-

Table 1. Database used in analysis

Database	Website
NCBI	http://www.ncbi.nlm.nih.gov
Gene Database goat	http://goat.kiz.ac.cn/GGD/
EMBOSS Nc value	http://emboss.bioinformatics.nl/cgi-bin/emboss/chips
EMBOSS CUSP	http://emboss.bioinformatics.nl/cgi-bin/emboss/cusp
EMBOSS CA	http://emboss.bioinformatics.nl/cgi-bin/emboss/cai
SOPMA	http://npsa-pbil.ibcp.fr/cgibin/npsa_automat.pl?page=npsa_sopma.html
Swiss	http://swissmodel.expasy.org/
NCBI CD-search	http://www.ncbi.nlm.nih.gov/Structure/cdd/wrpsb.cgi
Pfam	http://pfam.janelia.org/search/sequence
SMART	http://smart.embl-heidelberg.de/
ProtFun	http://www.cbs.dtu.dk/services/ProtFun/

ware, using the cusp of each species (22). Ka/Ks was calculated by PAML 4.7 (23).

Alignment of the CD61 protein

Amino acid sequences were aligned with published sequences in GenBank by DNAMAN software. Secondary structures of CD61 proteins were analysed by SOPMA website. Motifs of CD61 protein were analysed by Gene Runner software. Predicted 3D model of human CD61 protein has been performed by SWISS website. Domains of CD61 protein of mouse and human were analysed by NCBI CD-Search, Pfam and SMART website. Hydrophobicity of CD61 protein of mouse and human were predicted by DNAMAN. Cellular role, enzyme class and Gene Ontology category of mouse and human CD61 proteins were predicted by Protfun program on CBS website**.**

Lentivirus preparation and cell transfection

Lentivirus was produced as described by Anokye-Danso *et al.* (24). Briefly, HEK293T cells were seeded on plates 24 h before transfection, then plasmid pCD61-CAGG-TRIP-pur with plasmids containing pVSVG and pPAX were incubated. Virus-containing supernatant was collected 48 h after transfection, filtered to remove cell debris, and prepared for transduction. Cells were plated at 1×10^5 cells in six-well plates. Twelve hours later, they were transduced with virus containing supernatant and 10 μg/ml polybrene (Sigma, San Francisco, CA, USA), and incubated overnight at 37 °C and 5% CO_2. After 24 h, medium was discarded and replaced with fresh.

hUC-MSC induction

The induction protocol refers to Li *et al.* (2014). Induction medium was made with 12.5 ng/ml human BMP4 (PeproTech, Rocky Hill, NJ, USA), in normal culture medium (13). For EB (embryoid bodies) formation, 2×10^5 cells were seeded into 35 mm plates with 1.5 ml culture medium. Cells were resuspended for 16 h, and EBs formed after a further 3 days. Appropriate EBs were added to 96-well plates and 12-well plates; after adherence overnight, culture medium was replaced with induction medium, which was changed every 2 days (17).

Immunofluorescence staining

Cells were fixed in 4% paraformaldehyde (PFA) for 10 min, then rinsed twice in PBS for 3 min. After treating with 0.1% Triton X-100 for 10 min at room temperature, they were then blocked in 1% BSA for 30 min; they were then incubated in primary antibody overnight. Primary antibodies were as follows: PRDM1 (mouse monoclonal, 1:400; Biolegend, San Diego, CA, USA), PRDM14 (rabbit polyclonal, 1:500; Sigma, San Francisco, CA, USA), SSEA-1 (mouse monoclonal, 1:100; Millipore, MA, USA) and CD61 (rabbit polyclonal, 1:200; Abcam, Cambridge, UK). After washing three times in PBS, they were incubated in fluorochrome-conjugated secondary antibody (1:500; Millipore) for 1 h at room temperature in the dark. HOECHST33342 (Sigma) was used to stain cell nuclei, 3 min at room temperature (RT), after being rinsed twice for 3 min in PBS. Cells were then examined using a fluorescence microscope (13,17).

Semi- quantitative RT-PCR and quantitative-RT-PCR analyses

Total RNAs for semi-quantitative RT-PCR and quantitative-RT-PCR (RT-qPCR) analyses were extracted from overexpressed CD6 l (oCD61) and Control (Con) using TRIzol (Tiangen Biotech Co. Ltd., Beijing, China). cDNAs were synthesized and reactions were set up in 15 μl reaction mixtures containing 7.5 μl 2× BioEasy SYBRGreen Mix (Bioer Technology, Hangzhou, China), 0.3 μl sense primers, 0.3 μl antisense primers, 6.6 μl distilled water, 0.5 μl template and 0.1 μl Taq DNA polymerase. Reaction conditions were as follows: 94 °C for 5 min, and then 40 cycles 94 °C for 20 s, 58 °C for 30 s and 70 °C for 10 s. All expression levels were normalized to GAPDH in each well. Double δCt method was used to measure relative gene expression. Fluorescence signal was collected every 0.5 °C for 10 s. RT-qPCR primers are listed in Table 2.

Statistical analysis

One-way analysis of variance (one-way ANOVA) was used and post-tests were conducted using Newman–Keuls multiple range test, if P values were significant. Student's t-test was used when only two pairs of data were compared. All data are represented as mean SD, and statistical significance is expressed as follows: $*P < 0.05$; $**P < 0.01$; $***P < 0.001$. All data are representative of at least three different experiments and were analysed using Graphpad Prism software (La Jolla, CA, USA).

Results

Cloning the human CD61 gene

To study the role of CD61 in hUC-MSCs, we cloned it from umbilical cord cDNA by PCR (Fig. 1a). Length of

Table 2. primer sequences

Gene name	Primer name	Primer sequence	Tm/°C
CD61	CD61F	GAGCCCATTTTCTTCTCCCG	58
	CD61R	GCAACACCATGAATCCATCCC	
PRDM1	PRDM1F	TGGAGGACGCTGATATGACT	58
	PRDM1R	GCTTGACACCGGGGTTTAG	
AP2γ	AP2γF	TGAAGATGAAGCTGGGCTTT	58
	AP2γR	TCCATTCTCTTCCGGTTCAG	
PRDM14	PRDM14F	ACAGCCAAGCAATTTGCACTAC	58
	PRDM14R	TTACCTGGCATTTTCATTGCTC	
SSEA-1	SSEA-1F	ACGGATAAGGCGCTGGTACTA	59
	SSEA-1R	GGAAGCCATAGGGCACGAA	
STELLA	STELLAF	GACCCAATGAAGGACCCTGAA	59
	STELLAR	GCTTGACACCGGGGTTTAG	
GAPDH	GAPDHF	TGGCCTTCCGTGTTCCTAC	58
	GAPDHR	GAGTTGCTGTTGAAGTCGCA	
STRA8	STRA8F	AGCAGCTTAGAGGAGGTCAAGA	57
	STRA8R	TACTCGGAACCTCACTTTTGTC	
C-KIT	C-KITF	TGACTTACGACAGGCTCGTG	58
	C-KITR	AAGGAGTGAACAGGGTGTGG	
PRM1	PRM1F	ATAGCACATCCACCAAACTCC	58
	PRM1R	AGGCGGCATTGTTCCTTAG	

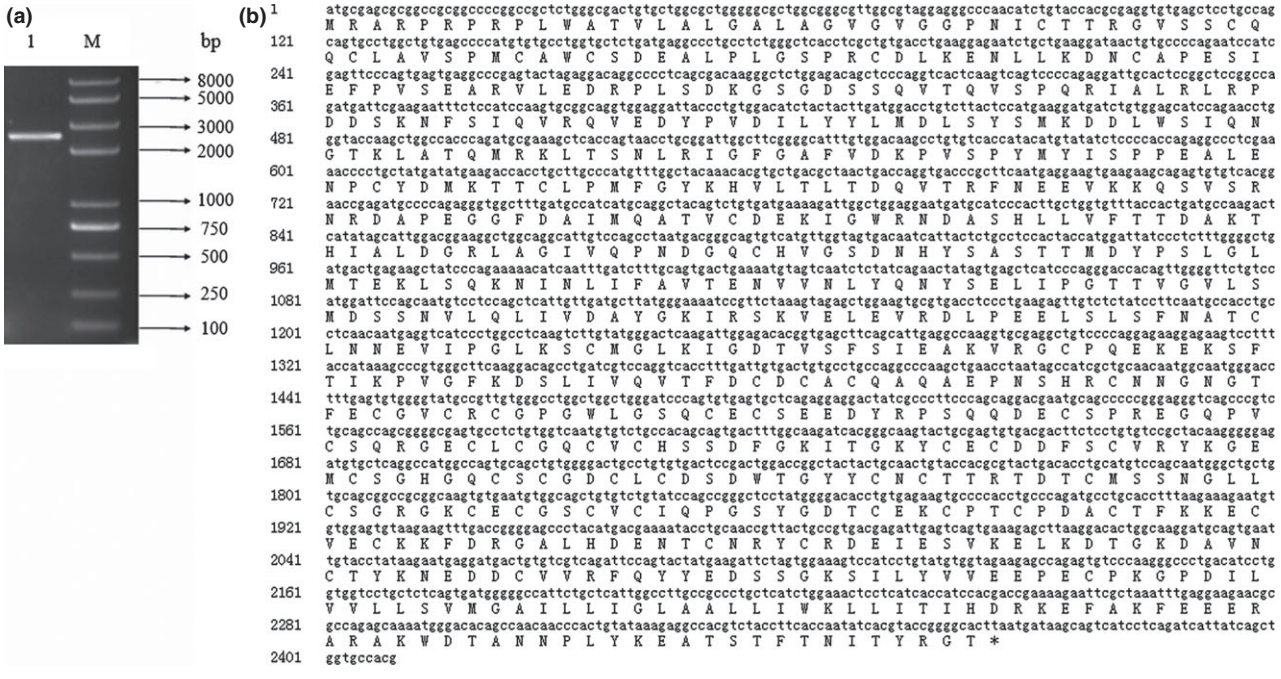

Figure 1. Sequence of the human *CD61* gene. (a) The CD61 was cloned. (b) Nucleotide and deduced amino acid sequence of human *CD61*.

the fragment we obtained was 2409 bp, containing CDS, partial 3'UTR of CD61 mRNA. The fragment was sequenced and showed the cloned human CD61 CDS to be of 2366 bp (Fig. 1b). The human *CD61* gene was located on chromosome 17, which was identified by NCBI blasting.

Homology comparison of CD61 CDS

We aligned sequencing results with other species CD61 CDS sequences by NCBI and DNAMAN, including *Homo sapien*, *Sus scrofa*, *Mus musculus*, *Rattus norvegicus*, *Gallus gallus*, *Bos taurus*, *Canis lupus*

familiaris and *Ovis arise*. The results showed the *CD61* gene is highly conserved. Human *CD61* was found to be homologous with *Canis lupus familiaris* and some cloven-hoofed mammals, sharing 90.83% homology with that of *Canis lupus familiaris*. These results indicated that human *CD61* shared a high level of homology with other species, and the phylogenetic tree was plotted (Table 3; Fig. 2a).

Analysis of the CD61 gene codon

Submitted *CD61* sequences were analysed using the EMBOSS website (Table 4) which performed the calculation of codon bias with its online program chips; the calculation result was given by Nc (effective number of codon) value. Nc value is the number of types of codons used in a gene; its value is generally between 20 (each amino acid only use one codon) and 61 (each codon be used averagely). These results showed that Nc values of these species were all in the range 40.653–48.052. Nc value of non-mammals is a little lower than that of mammals. Analysis of amino acid codon bias index (CBI) and codon adaptation index (CAI) suggested that CBI and CAI were not significantly different between different species (Table 5). These results also supported the notion that the *CD61* gene is conserved.

In genetics, the ratio of non-synonymous substitutions per non-synonymous site (Ka) to number of syn-

Table 3. Comparison of length of CD61 in CDS and amino acid

Species	Length of CDS	Length of amino acid	Homology (%)
Homo sapien	2367	789	100
Sus scrofa	2355	785	89.82
Mus musculus	2364	788	86.52
Rattus norvegicus	2364	788	86.95
Gallus gallus	2346	782	77.09
Bos Taurus	2355	785	90.11
Canis lupus familiaris	2355	785	90.83
Ovis aries	2424	808	88.70

Table 4. N_c value of CD61 gene

Species	Nc values
Homo sapiens	48.052
Sus scrofa	46.250
Mus musculus	46.781
Rattus norvegicus	46.659
Gallus gallus	40.653
Bos taurus	46.515
Canis lupus familiaris	47.324
Ovis aries	45.720

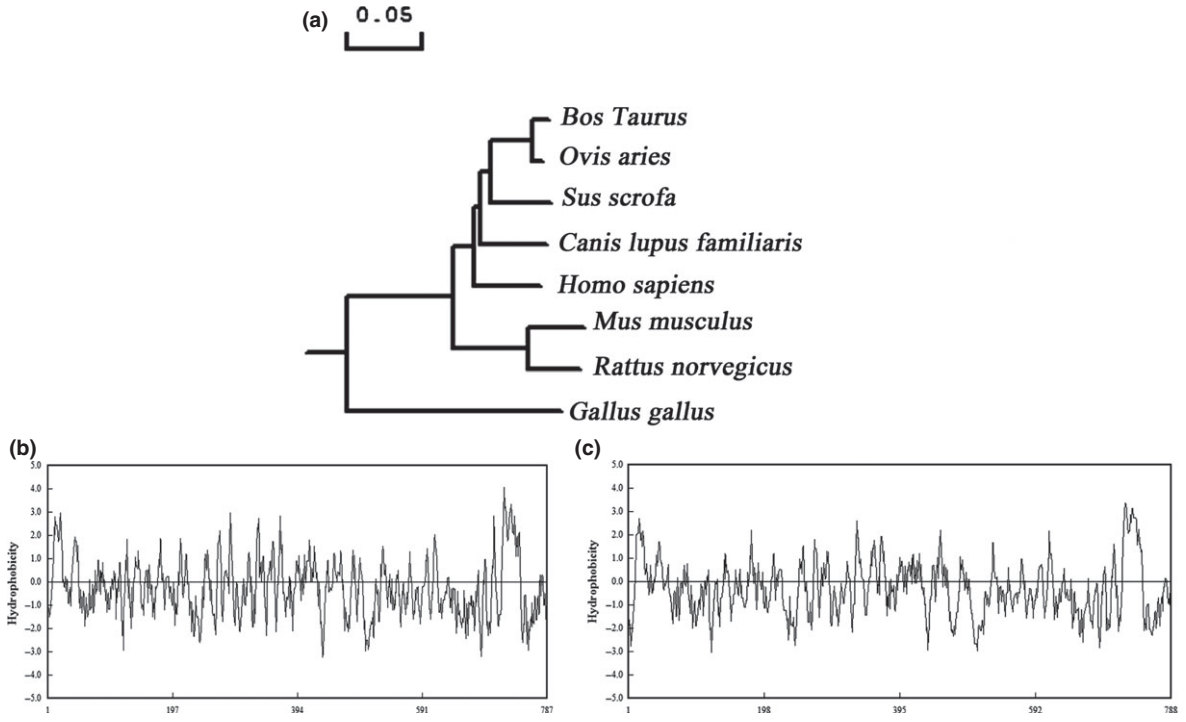

Figure 2. Characteristics of *CD61*. (a) Phylogenetic trees of *CD61* gene. Prediction of hydrophobicity of (b) mouse CD61 protein and (c) human CD61 protein.

Table 5. CBI and CAI of CD61 gene

Species	CAI	CBI
Homo sapien	0.804	0.348204601104916
Sus scrofa	0.818	0.414000758792688
Mus musculus	0.817	0.357809579132719
Rattus norvegicus	0.815	0.368624807777598
Gallus gallus	0.850	0.528126682396996
Bos Taurus	0.818	0.414144918157355
Canis lupus familiaris	0.808	0.377792963889501
Ovis aries	0.817	0.422189379888813

Table 6. Secondary structure analysis of CD61 protein

Species	Alpha helix	Extended strand	Beta turn	Random coil
Homo sapien	213	173	78	324
Sus scrofa	193	186	84	321
Mus musculus	215	181	81	310
Rattus norvegicus	215	183	81	308
Gallus gallus	224	182	79	296
Bos Taurus	212	179	78	315
Canis lupus familiaris	210	181	80	313
Ovis aries	215	179	78	333

onymous substitutions per synonymous site (Ks) can be used as an indicator of selective pressure acting on a protein-coding gene (25). Our results prove that Ka/Ks values of all the groups were lower than 1 (Fig. S1), indicating that non-synonymous substitutions are less than synonymous ones in the CD61 protein; that it is evolutionarily conserved.

Sequence analysis of CD61 protein between different species

Amino acid sequences of different species have been aligned by DNAMAN software (Fig. S2) and results revealed that CD61 protein is also highly conserved, with total identity of 89.11%.

Secondary structure of different species is predicted by SOPMA (Table 6) and amount of α-helix was 193–224. Extended strand is 173–186 and β-turn is 78–84, while random coil is 296–333. Amounts of components in each kind of protein were similar, indicating that CD61 protein is evolutionarily conserved.

By motif analysis, we found that some sites of CD61 have changed little (Table 7), such as sites of aldehyde dehydrogenases cysteine activity, cAMP phosphorylation, epidermal growth factor-like (EGF-like

Table 7. Motif analysis of CD61 protein

Species	Aldehyde dehydrogenases site	cAMP phosphorylation site	EGF	Glycosaminoglycan	Integrin beta	Asn glycosylation
Homo Sapien	555	469	486	563 602	521	125 346 397
		234	573		562	478
					601	585 680 782
Sus Scrofa	551	165	482	559 598	517	233 342 358
			569		550	393
					597	474 581 676
						778
Mus musculus	554	168	485	562 601	520	345 396 477
		233	572		561	584
					600	679 781
Rattus norvegicus	554	168	485	562 601	520	345 396 477
		233	572		561	584
					600	679 781
Gallus gallus	547	161	478	555 594	513	338 309 452
		226	565		554	462
					593	470 577 672
						774
Bos taurus	551	165	482	559 590	517	342 393 474
		230	569		558	581
					597	676 778
Canis lupus familiaris	551	230	482	559	517	121 342 393
			569		558	474
					597	581 676 778
Ovis aries	574	188	505	582 621	540	365 416 497
		253	592		581	604
					620	699 801

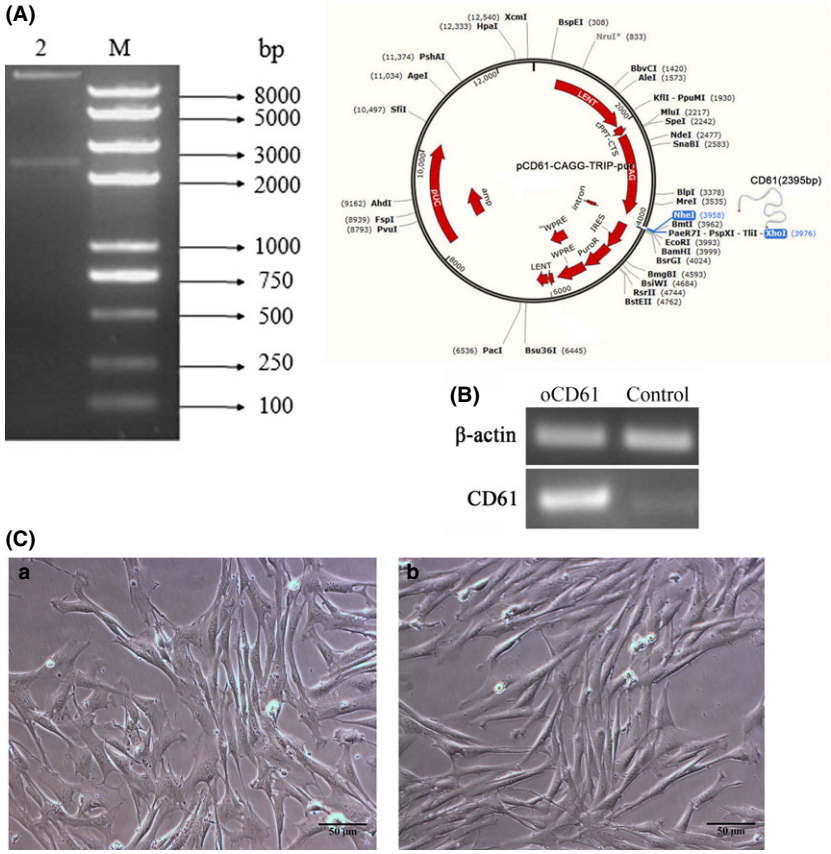

Figure 3. Overexpression of CD61 in hUC-MSCs. (A) The pCD61-CAGG-TRIP-pur recombination plasmid was verified by NheI and XhoI double digestion. (B) Expression level of CD61 in pCD61-CAGG-TRIP-pur transduction group was significantly higher than that in the pTRIP-CAGG-pur group; the results are shown by semi-quantitative RT-PCR. (C) Morphology of hUC-MSCs transducted by CD61. (a) hUC-MSCs cultured in normal culture medium before transduction. (b) Figuration of hUC-MSCs after transducted for 2 days.

domain cysteine pattern signature), glycosaminoglycan attachment, N-glycosylation and of integrin-β chain cysteine-rich domain signature. The integrin-β chain cysteine-rich domain signature region is the main functional site. Whether other binding regions are functional has yet to be verified.

Hydrophobicity of a protein is the fundamental element of its structure. In this study hydrophobicity of human and *Mus musculus* CD61 protein were analysed (Fig. 2b,c) and results indicated that human CD61 protein and that of *Mus musculus* share analogous hydrophobicity. Their 3' and 5'ends have hydrophilic and hydrophobicity characteristics respectively, implying that the structure of CD61 protein has not changed greatly over long evolutionary history.

CD61 regulated hUC-MSCs to differentiate into PGC-like cells

To test the effects of CD61 on hUC-MSC differentiation, plasmids pCD61-CAGG-TRIP-pur and pTRIP-CAGG-pur (Control) were transduced into hUC-MSCs (Fig. 3A). According to semi-quantitative RT-PCR and western blotting, pCD61-CAGG-TRIP-pur was successfully transduced into hUC-MSC (Figs. 3B, 4C). Cell morphology changed after transduction: the hUC-MSCs formed spindle fibroblast-like phenotypes or were irregular in shape (Fig. 3C-a); after being transduced with pCD61-CAGG-TRIP-pur for 48 h, they became thinner or round (Fig. 3C-b).

To test whether those thinner-shaped cells were PGCs, RT-qPCR and immunofluorescence staining were conducted to assess expressions of PGC-specific markers, at both mRNA and protein levels, including SSEA1, PRDM1, PRDM14, AP2γ, SOX2 and C-KIT; results showed that these PGC markers were increased by CD61 overexpression (Fig. 4A,B).

hUC-MSCs overexpressing CD61 differentiated into male germ-like cells under BMP4 induction

A previous study by our group has demonstrated that BMP4 can be responsible for differentiation of hUC-MSCs (13). Thus, we tried to induce hUC-MSC-CD61 (CD61-overexpressing hUC-MSCs) and hUC-MSCs (Control group cells transduced with empty plasmid) with BMP4. After 7 days, the configuration of hUC-MSCs-CD61 cells was altered; round-shaped cells and

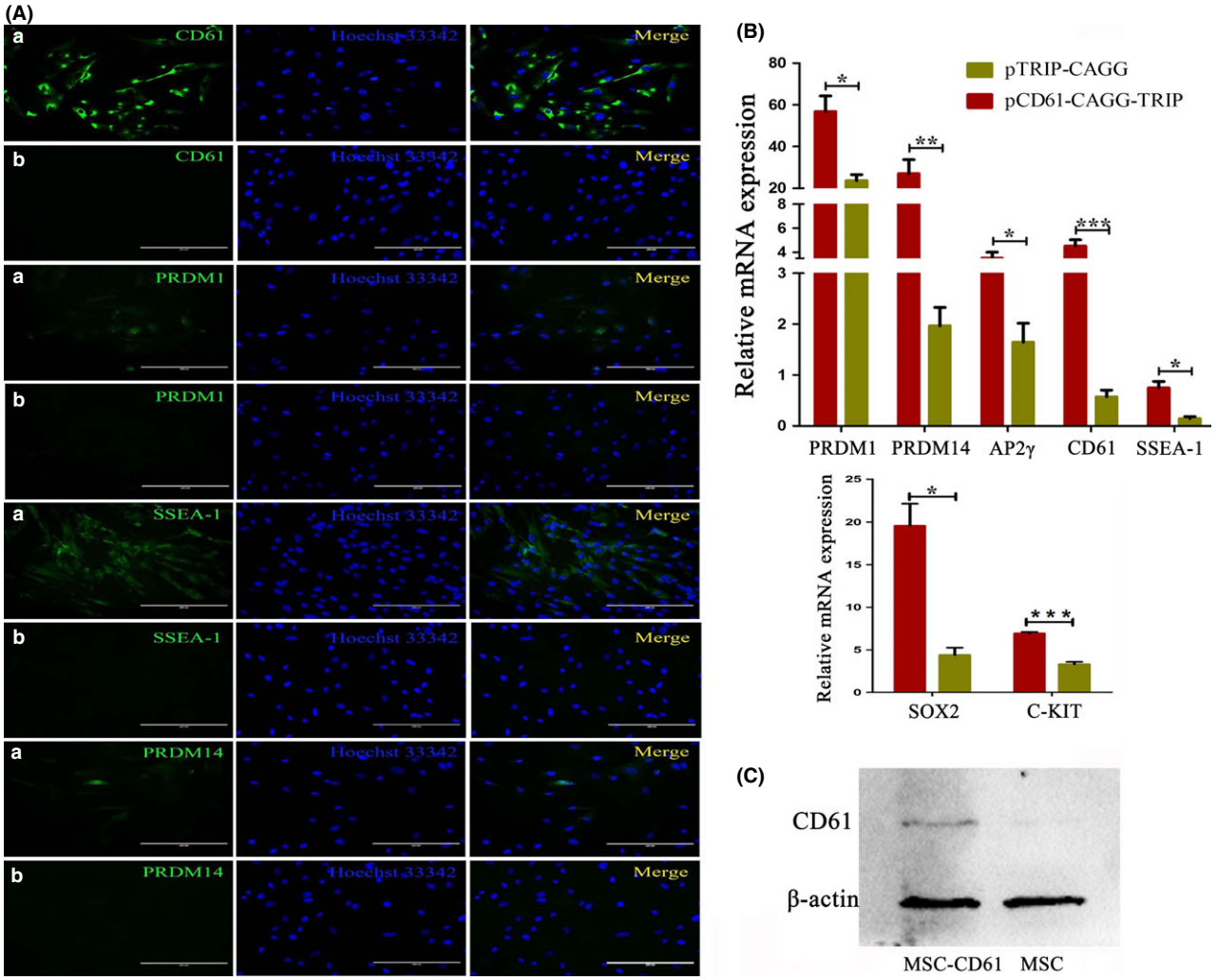

Figure 4. hUC-MSCs overexpressing CD61 differentiated into PGC-like cells. (A) Immunofluorescence staining of expression levels of CD61, SSEA-1, PRDM1 and PRDM14 in hUC-MSC-CD61 (a) and hUC-MSC cells (b). (B) RT-qPCR analysis results of hUC-MSC-CD61 and hUC-MSC cells: both expressed mRNAs of the above genes but with differences in quantities. Expression levels of AP2γ, PRDM1, PRDM14, SOX2, C-KIT, SSEA-1 and CD61 in hUC-MSC-CD61 cells were significantly higher than those in hUC-MSC cells. (C) Expression of CD61 increased in hUC-MSC-CD61 compared to hUC-MSC cells (Control), analysed by western blotting. $*P < 0.05$; $**P < 0.01$; $***P < 0.001$

spermatid-like cells with tails could occasionally be seen (Fig. 5A-a), while no changes in morphology were observed in the of Control group (Fig. 5A-b). Compared to hUC-MSCs, expression levels of Scp3, Stra8 and Prm1 in hUC-MSCs-CD61 significantly increased when induced by BMP4 (Fig. 5B). Induced spermatid-like cells were positive for ACR. In combination with the previous study, our experiments showed that BMP4 induced hUC-MSCs to differentiate into PGC-like cells; furthermore, BMP4 induced CD61-overexpressing hUC-MSC differentiation into male germ-like cells. Thus, we confirmed that overexpression of CD61 promoted hUC-MSCs to transdifferentiate into PGC-like cells, and then differentiate towards male germ-like cells under BMP4 induction.

Discussion

Integrins compose a membrane receptor family, widely found in cells and tissues. It identifies arginine–glycine–aspartate (Arg-Gly-Asp, RGD) sequence of ligands and mediates interactions, not only within cells, but also between cells and the extracellular matrix (26), which are dependent on Ca^{2+} regulation (27). The integrin ligand is an extracellular matrix component, involved in embryonic development, immunologi-

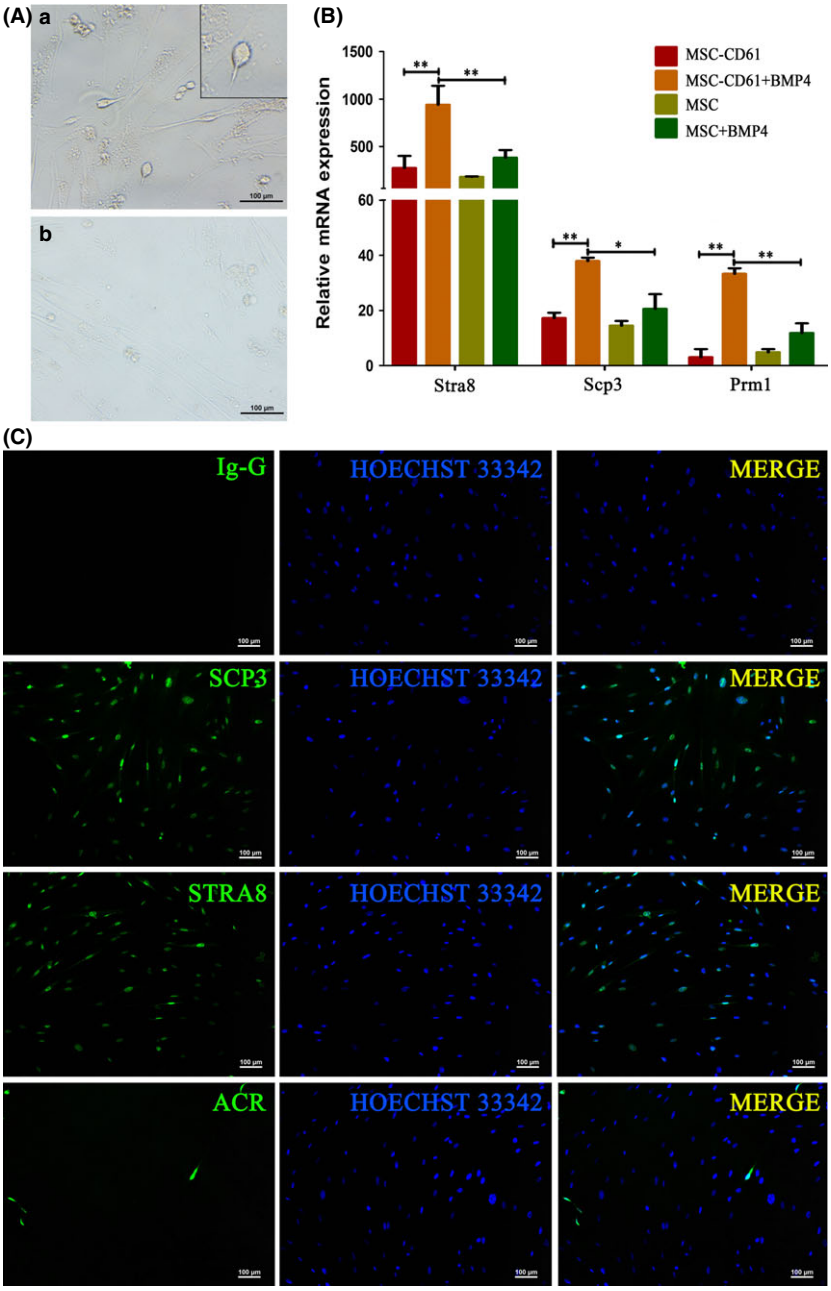

Figure 5. Analysis of male germ cell-specific markers. (A) After being induced by BMP4, spermatid-like cells were produced in hUC-MSC-CD61 cells (red arrow). (B) RT-qPCR analysis showed that expression levels of STRA8, SCP3 and PRM1 in the CD61 transducted group were higher than those of the Control group. (C) Immunofluorescence assay presented the same results; also, ACR positive cells were formed. $*P < 0.05$; $**P < 0.01$; $***P < 0.001$

cal response, wound healing, malignant tumour metastasis and in many further important physiological and pathological processes (28,29). Recent study has found that integrin-β3 is associated with breast cancer invasion and metastasis of malignant progression (30). Furthermore, integrin-β3 protein may be involved in the p38 MAPK signalling pathway, which regulates cell growth, apoptosis, movement and the invasive phenotype (31).

Human integrin-β3 was cloned and analysed at both nucleic acid and protein levels with modern bioinformatics software as well as utilization of websites. Results show that human CD61 nucleic acid sequence is highly conserved, consistent with species phylogenetic relationships. Codon usage preference is related to co-workers tRNA concentration, thus contributes to efficiency and accuracy of translation (32). Codon selection mode in single-celled evolutionary processes is conserved. Multicellular organisms, especially mammals, however, are not the same. They use fewer co-workers tRNA to control protein synthesis, and to improve accuracy of protein synthesis, where high energy is consumed, by

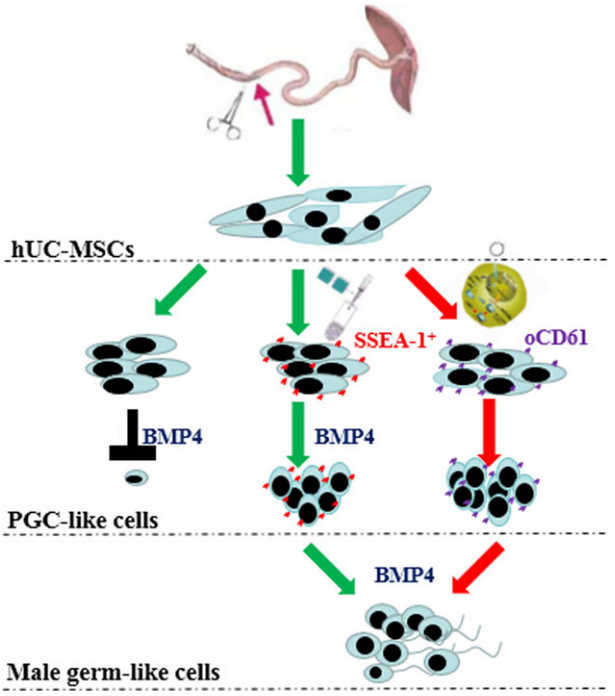

Figure 6. Schematic of induction of hUC-MSCs to differentiate into male germ-like cells. Overexpression of CD61 caused differentiation of hUC-MSCs into PGC-like cells, in which PGC-related markers were detected. When the above cells and SSEA-1$^-$positive hUC-MSC cells were treated by BMP4, expression of meiotic markers, ACR, STRA8 and SCP3 were markedly increased. Male germ-like cells were obtained.

reducing synthesis speed (33). The reason for integrin-β3 codon bias evolution may lie in availability of tRNA, or in abundance of the tRNA in the developmental process. Analysis of Ka/Ks revealed that *integrin-β3* gene codon bias is quite conservative over the course of evolution, demonstrating that this gene is essential for all organisms. With the seemingly increasing rate of male infertility, more and more attention has been drawn to trans-differentiation, and efforts to induce other types of cells to become germ cells. Although several studies have shown that besides mouse and human embryonic cells, adult stem cells and induced pluripotent stem cells (iPSCs) also, have some capacity to differentiate into germ-like cells *in vivo* or *in vitro* (5–7,34–37), adult stem cells and iPSCs are difficult to obtain, and adult stem cells are limited in their pluripotency, not sufficient to be used to investigate the germ cell development. Otherwise, compared to other adult stem cells, hUC-MSCs are 'younger' and easier to obtain, and in addition, are able to differentiate into a variety of cell types (2,8,11). hUC-MSCs can differentiate into germ cells when transplanted into seminiferous tubules of mice treated with busulfan (2,38). The cells have been reported exhibit round cell shapes typical of proliferating/differentiating germ cells, and to express germ cell markers OCT4, C-KIT and VASA (37,39).

Germ cell lineage primordial germ cells (PGCs) in mammals originate from the pluripotent epiblast and undergo sexually dimorphic development, generating spermatozoa in males (3). Integrin-β3- and SSEA1-positive cells are close to BV-positive cells, which have been verified to be PGC cells (3); SSEA-1$^+$ hUC-MSC can differentiate into PGC-like cells (13). In our work, integrin-β3 was overexpressed in hUC-MSCs and 2 days later, some spherical PGC-like cells appeared. Further analysis revealed that levels of PGC-specific markers, SSEA-1, PRDM1, PRDM14, AP2γ, STELLA, SOX2 and C-KIT, were up-regulated (13,19,21,40). In view of these pieces of evidence, we postulate that overexpressing-CD61 hUC-MSCs were indeed, PGC-like cells.

BMP4 is a specific cytokine which can promote ESC differentiation to PGCs *via* activating the Smad1/5/8 signalling pathway (41,42). BMP4 facilitates phosphorylation of receptor-regulated Smads and subsequently binds to cooperating Smad1/5/8 and Smad4. Smad complexes are then translocated to the nucleus and activate transcription of BMP target genes, including germ cell-related genes (43). Under BMP4 induction, SSEA-1+ hUC-MSCs easily transdifferentiate into PGC-like cells, then differentiate into male germ-like cells (13). *SCP3* is a meiosis-related gene which participates in formation of the synaptonemal complex (44), while STRA8 is viewed as the first putative marker representing the switch to meiosis of mammalian stem cells (45). Prm1 is the specific marker of the post-meiotic spermatids (6). In our study, expression levels of the above germ cell markers were up-regulated significantly in CD61-hUC-MSCs treated with 12.5 ng/ml BMP4 for 7 days, and even some spermatid-like cells were observed and positive for spermatid marker-ACR. Immunofluorescence staining further indicated that the percentage of ACR-positive cells increased (5). These results further support that, under induction of BMP4, CD61-overexpressing hUC-MSCs were induced into differentiation into male germ-like cells.

Notably, compared to hUC-MSCs cultured in normal medium, such cells cultivated in medium to which BMP4 had been added expressed more Stra8, Scp3 and Prm1 at the transcriptional level while still not being able to differentiate into male germ-like cells, indicating that BMP4 promotes expression of PGC and meiosis-related genes, and efficiency of promotion is unremarkable. However, it is not the same with hUC-MSCs overexpressing CD61, which have shown similar characteristics of PGCs (7,46). In these cells, meiosis-related genes were up-regulated not only at transcriptional level but

also at protein level, demonstrated by male germ-like cells with tails as well as with positive immunofluorescence staining results. The effect of BMP4 in promoting hUC-MSC differentiation into germ-like cells is limited when alone, however, it worked well for cells with PGC-specific markers. Our results reveal that CD61 and BMP4 exerted their potentials in different phases of the trans-differentiation process from hUC-MSCs to germ-like cells (Fig. 6), while CD61 promoted hUC-MSC transdifferentiation into PGCs, in combination with BMP4, and enhanced cell differentiation into male germ-like cells.

Taken together, our work demonstrates that combination of CD61 overexpression with BMP4 induced efficient hUC-MSC differentiation into male germ-like cells (Fig. 6). When CD61 succeeds in transformation of hUC-MSCs into PGC-like cells, BMP4 induces such PGC cells differentiate into male germ-like cells in a further step.

Acknowledgements

This work was supported by grants from the Program of National Natural Science Foundation of China (31272518, 31572399), National High Technology Research and Development Program of China (SS2014AA021605), the Key Project of Chinese Ministry of Science and Technology (2013CB967401), Doctoral Fund of Ministry of Education of China (RFDP, 20120204110030), and the Program of the Shaanxi Province (2015NY157).

References

1 Hargreave TB (2000) Genetic basis of male fertility. *Br. Med. Bull.* **56**, 650–671.
2 Chen H, Tang QL, Wu XY, Xie LC, Lin LM, Ho GY *et al.* (2015) Differentiation of human umbilical cord mesenchymal stem cells into germ-like cells in mouse seminiferous tubules. *Mol. Med. Rep.* **12**, 819–828.
3 Hayashi K, Ogushi S, Kurimoto K, Shimamoto S, Ohta H, Saitou M (2012) Offspring from oocytes derived from *in vitro* primordial germ cell-like cells in mice. *Science* **338**, 971–975.
4 Hayashi K, Ohta H, Kurimoto K, Aramaki S, Saitou M (2011) Reconstitution of the mouse germ cell specification pathway in culture by pluripotent stem cells. *Cell* **146**, 519–532.
5 Vilagran I, Castillo J, Bonet S, Sancho S, Yeste M, Estanyol JM *et al.* (2013) Acrosin-binding protein (ACRBP) and triosephosphate isomerase (TPI) are good markers to predict boar sperm freezing capacity. *Theriogenology* **80**, 443–450.
6 Nayernia K, Nolte J, Michelmann HW, Lee JH, Rathsack K, Drusenheimer N *et al.* (2006) In vitro-differentiated embryonic stem cells give rise to male gametes that can generate offspring mice. *Dev. Cell* **11**, 125–132.
7 Cooke PS, Nanjappa MK (2015) How to make a human germ cell. *Asian J. Androl.* **17**, 441–442.
8 Lian MA, Xue-yong F, Bing-lin C, Law F, Xue-wu J, Li-ye Y *et al.* (2005) Human umbilical cord Wharton's Jelly-derived mesenchymal stem cells differentiation into nerve-like cells. *Chin. Med. J. (Engl)* **118**, 1987–1993.
9 Kee K, Gonsalves JM, Clark AT, Pera RA (2006) Bone morphogenetic proteins induce germ cell differentiation from human embryonic stem cells. *Stem Cells Dev.* **15**, 831–837.
10 Qiu P, Bai Y, Liu C, He X, Cao H, Li M *et al.* (2012) A dose-dependent function of follicular fluid on the proliferation and differentiation of umbilical cord mesenchymal stem cells (MSCs) of goat. *Histochem. Cell Biol.* **138**, 593–603.
11 Hua J, Pan S, Yang C, Dong W, Dou Z, Sidhu KS (2009) Derivation of male germ cell-like lineage from human fetal bone marrow stem cells. *Reprod. Biomed. Online* **19**, 99–105.
12 Nayernia K, Lee JH, Drusenheimer N, Nolte J, Wulf G, Dressel R *et al.* (2006) Derivation of male germ cells from bone marrow stem cells. *Lab. Invest.* **86**, 654–663.
13 Li N, Pan S, Zhu H, Mu H, Liu W, Hua J (2014) BMP4 promotes SSEA-1(+) hUC-MSC differentiation into male germ-like cells in vitro. *Cell Prolif.* **47**, 299–309.
14 Hua J, Yu H, Dong W, Yang C, Gao Z, Lei A *et al.* (2009) Characterization of mesenchymal stem cells (MSCs) from human fetal lung: potential differentiation of germ cells. *Tissue Cell* **41**, 448–455.
15 Cao H, Chu Y, Zhu H, Sun J, Pu Y, Gao Z *et al.* (2011) Characterization of immortalized mesenchymal stem cells derived from foetal porcine pancreas. *Cell Prolif.* **44**, 19–32.
16 Li DF, Zhang MC, Yang HJ, Zhu YB, Xu X (2007) Beta-integrin mediates WSSV infection. *Virology* **368**, 122–132.
17 Trubner M, Glander HJ, Schaller J (1997) Localization of adhesion molecules on human spermatozoa by fluorescence microscopy. *Andrologia* **29**, 253–260.
18 Hayashi K, Ogushi S, Kurimoto K, Shimamoto S, Ohta H, Saitou M (2012) Offspring from oocytes derived from in vitro primordial germ cell-like cells in mice. *Science* **338**, 971–975.
19 Dudley BM, Runyan C, Takeuchi Y, Schaible K, Molyneaux K (2007) BMP signaling regulates PGC numbers and motility in organ culture. *Mech. Dev.* **124**, 68–77.
20 Mazaheri Z, Movahedin M, Rahbarizadeh F, Amanpour S (2011) Different doses of bone morphogenetic protein 4 promote the expression of early germ cell-specific gene in bone marrow mesenchymal stem cells. *In Vitro Cell. Dev. Biol. Anim.* **47**, 521–525.
21 Li JF, Yin HL, Shuboy A, Duan HF, Lou JY, Li J *et al.* (2013) Differentiation of hUC-MSC into dopaminergic-like cells after transduction with hepatocyte growth factor. *Mol. Cell. Biochem.* **381**, 183–190.
22 Morton BR (1993) Chloroplast DNA codon use: evidence for selection at the psb A locus based on tRNA availability. *J. Mol. Evol.* **37**, 273–280.
23 Yang Z, Nielsen R (2000) Estimating synonymous and nonsynonymous substitution rates under realistic evolutionary models. *Mol. Biol. Evol.* **17**, 32–43.
24 Anokye-Danso F, Trivedi CM, Juhr D, Gupta M, Cui Z, Tian Y *et al.* (2011) Highly efficient miRNA-mediated reprogramming of mouse and human somatic cells to pluripotency. *Cell Stem Cell* **8**, 376–388.
25 Li J, Zhang Z, Vang S, Yu J, Wong GK, Wang J (2009) Correlation between Ka/Ks and Ks is related to substitution model and evolutionary lineage. *J. Mol. Evol.* **68**, 414–423.
26 Nanda SY, Hoang T, Patel P, Zhang H (2014) Vinculin regulates assembly of talin: beta3 integrin complexes. *J. Cell. Biochem.* **115**, 1206–1216.

27 Lafrenie RM, Yamada KM (1996) Integrin-dependent signal transduction. *J. Cell. Biochem.* **61**, 543–553.
28 Bojesen SE, Kjaer SK, Hogdall EV, Thomsen BL, Hogdall CK, Blaakaer J *et al.* (2005) Increased risk of ovarian cancer in integrin beta3 Leu33Pro homozygotes. *Endocr. Relat. Cancer* **12**, 945–952.
29 Reuning U (2011) Integrin alphavbeta3 promotes vitronectin gene expression in human ovarian cancer cells by implicating rel transcription factors. *J. Cell. Biochem.* **112**, 1909–1919.
30 Hong IK, Kim YM, Jeoung DI, Kim KC, Lee H (2005) Tetraspanin CD9 induces MMP-2 expression by activating p38 MAPK, JNK and c-Jun pathways in human melanoma cells. *Exp. Mol. Med.* **37**, 230–239.
31 Cardone RA, Bagorda A, Bellizzi A, Busco G, Guerra L, Paradiso A *et al.* (2005) Protein kinase A gating of a pseudopodial-located RhoA/ROCK/p38/NHE1 signal module regulates invasion in breast cancer cell lines. *Mol. Biol. Cell* **16**, 3117–3127.
32 Ikemura T (1985) Codon usage and tRNA content in unicellular and multicellular organisms. *Mol. Biol. Evol.* **2**, 13–34.
33 Lavner Y, Kotlar D (2005) Codon bias as a factor in regulating expression via translation rate in the human genome. *Gene* **345**, 127–138.
34 Kee K, Angeles VT, Flores M, Nguyen HN, Reijo PR (2009) Human DAZL, DAZ and BOULE genes modulate primordial germ-cell and haploid gamete formation. *Nature* **462**, 222–225.
35 Hu Y, Sun J, Wang J, Wang L, Bai Y, Yu M *et al.* (2012) Characterization of female germ-like cells derived from mouse embryonic stem cells through expression of GFP under the control of Figla promoter. *J. Cell. Biochem.* **113**, 1111–1121.
36 Lv X, Zhu H, Bai Y, Chu Z, Hu Y, Cao H *et al.* (2012) Reversine promotes porcine muscle derived stem cells (PMDSCs) differentiation into female germ-like cells. *J. Cell. Biochem.* **113**, 3629–3642.
37 Huang P, Lin LM, Wu XY, Tang QL, Feng XY, Lin GY *et al.* (2010) Differentiation of human umbilical cord Wharton's jelly-derived mesenchymal stem cells into germ-like cells *in vitro*. *J. Cell. Biochem.* **109**, 747–754.
38 Nejad NA, Amidi F, Hoseini MA, Nia KN, Habibi M, Kajbafzadeh AM *et al.* (2015) Male germ-like cell differentiation potential of human umbilical cord Wharton's jelly-derived mesenchymal stem cells in co-culture with human placenta cells in presence of BMP4 and retinoic acid. *Iran J. Basic Med. Sci.* **18**, 325–333.
39 Mauduit C, Hamamah S, Benahmed M (1999) Stem cell factor/c-kit system in spermatogenesis. *Hum. Reprod. Update* **5**, 535–545.
40 Vincent JJ, Li Z, Lee SA, Liu X, Etter MO, Diaz-Perez SV, *et al.* (2011) Single cell analysis facilitates staging of Blimp1-dependent primordial germ cells derived from mouse embryonic stem cells. *PLoS ONE* **6**, e28960.
41 Kee K, Gonsalves JM, Clark AT, Pera RA (2006) Bone morphogenetic proteins induce germ cell differentiation from human embryonic stem cells. *Stem Cells Dev.* **15**, 831–837.
42 Bai H, Gao Y, Arzigian M, Wojchowski DM, Wu WS, Wang ZZ (2010) BMP4 regulates vascular progenitor development in human embryonic stem cells through a Smad-dependent pathway. *J. Cell. Biochem.* **109**, 363–374.
43 Murakami G, Watabe T, Takaoka K, Miyazono K, Imamura T (2003) Cooperative inhibition of bone morphogenetic protein signaling by Smurf1 and inhibitory Smads. *Mol. Biol. Cell* **14**, 2809–2817.
44 Syrjanen JL, Pellegrini L, Davies OR (2014) A molecular model for the role of SYCP3 in meiotic chromosome organisation. *Elife* DOI: 10.7554/eLife.02963.
45 Zhou Q, Li Y, Nie R, Friel P, Mitchell D, Evanoff RM *et al.* (2008) Expression of stimulated by retinoic acid gene 8 (Stra8) and maturation of murine gonocytes and spermatogonia induced by retinoic acid in vitro. *Biol. Reprod.* **78**, 537–545.
46 Irie N, Weinberger L, Tang WW, Kobayashi T, Viukov S, Manor YS *et al.* (2015) SOX17 is a critical specifier of human primordial germ cell fate. *Cell* **160**, 253–268.

Supporting Information

Additional Supporting Information may be found in the online version of this article:

Fig. S1 Ka/Ks analysis of CD61 in different species.

Fig. S2 Amino acid sequence alignment of CD61 in different species.